Two Views of the Cold Filament

GEORGES L. WEATHERLY AND EDWARD A. KELLEY, JR.‡

Department of Oceanography, Florida State University, Tallahassee, FL 32306

(Manuscript received 16 May 1983, in final form 18 July 1984)

ABSTRACT

Two views of the Cold Filament, first described by Weatherly and Kelley, are presented. The first is a local view near 40°N, 62°W. There its upslope edge is found to be a front which by benthic standards is large (its downslope edge was not sampled). What distinguishes this benthic front from others is that it is a permanent feature in the abyssal ocean. Above the Cold Filament, relatively murky detached bottom layers were observed and tracked to where they separated from the bottom at the benthic front. Apparently these detached layers entrain overlying water (a density jump at their base apparently restricts entrainment of underlying water) primarily during the detachment process with comparably less entrainment thereafter. The second view, a regional one, comes from examining historical hydrographic sections. These indicate that the Cold Filament extends from the Newfoundland Ridge westward then southward to 24°N and possibly to ~20°N along the base of the continental rise. The Cold Filament is postulated to be a part of an abyssal western boundary current in the North American Basin associated with a southern source of Antarctic Bottom Water.

1. Introduction

Weatherly and Kelley (1982) (hereafter referred to as WK) reported on an unexpected feature found above the bottom at the base of the continental rise south of Nova Scotia. It is seen in Fig. 1 (from WK) as an anomalously cold bottom layer of width ~ 100 km and thickness ~ 60 m, centered about the 4900 m isobath. Weatherly and Kelly found it in six hydrographic transects made in September–October 1979 and in two transects made in October 1980 as well as in historical sections made in the same region. Based on 8-month current meter velocity and temperature measurements made in and above it, WK concluded that it was not a pool or lens of colder water but rather a nearly continuous filament of colder water which flows equatorward at about 10 cm s^{-1} along isobaths, imbedded in the overlying fluid. They called this feature the Cold Filament, and by examining historical sections concluded it extended from about 50°W to at least 72°W along the base of the continental rise. This study was prompted by and is an extension of the work reported in WK. It is concerned with two distinct aspects of the Cold Filament. The first considers its local structure as revealed by a survey of one small portion of it. The second considers and tries to account for its geographical distribution in the western North Atlantic.

In Section 2 new data from one region at the base of the Scotian Rise are used to examine the following questions. Was the Cold Filament again there? If so, are its borders or edges as broad as indicated in Fig. 1 or are they sharper and more front-like? Is there regularity in the spatial variability of its bottom layer thickness and, if so, why? Is there evidence of bottom layer detachment from the sea floor at the borders of the Cold Filament as suggested by WK?

Historical hydrographic sections not examined by WK are used in Section 3: 1) to see if they are in agreement with the hypothesis of WK that the Cold Filament extends along the continental rise from 50 to 72°W and 2) to see if the Cold Filament extends farther south along the western border of the North American Basin. In Section 4 an abyssal circulation scheme is proposed to account for the distribution of the Cold Filament seen in Section 3.

2. Local survey of the cold filament

a. Background

As part of the site selection phase of the High Energy Benthic Boundary Layer Experiments (HEBBLE) program, a detailed bottom survey was made in June 1981 (Shor and Lonsdale, 1981) using the deeptow system (Spiess and Mudie, 1970). The data considered here were obtained during this survey along the dotted "zigzag" curve in Fig. 2. This curve is the path of the deeptow system as it was towed nominally 10 m above the bottom (mab). The up- and downslope extent of the survey covered approximately the expected upslope half of the Cold Filament and began upslope of its shoreward boundary (Fig. 1).

During the survey the deeptow system included a CTD (Neil Brown Instrument System, Falmouth,

‡ Present address: Department of Oceanography, Naval Postgraduate School, Monterey, CA 93943.

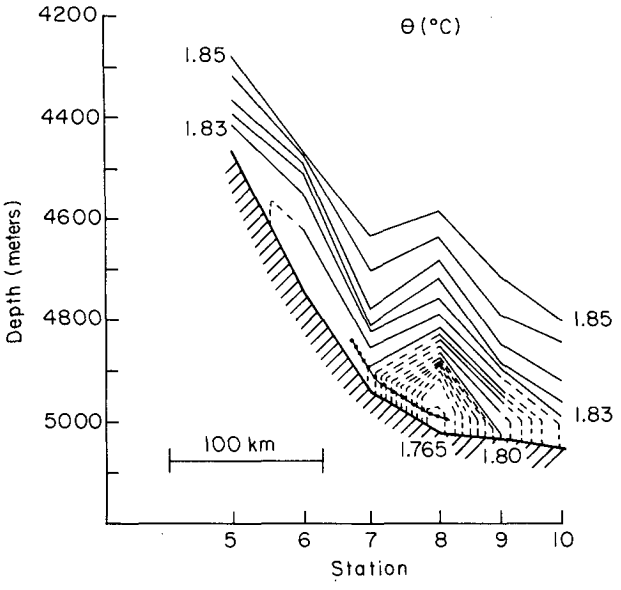

FIG. 1. Near-bottom potential temperature transect across the lower Scotian Rise (From Fig. 6 of WK). The Cold Filament is centered about the 5000 m isobath. Dotted solid line indicates across-rise track of deeptow survey.

Mass.) and a 25 cm pathlength, 660 nm light transmissometer (Sea Tech Corp., Corvallis, Oregon). Both were mounted below, forward and to one side of the deeptow main pressure housing so as to be unobstructed to the flow as the deeptow was towed forward. With the intent of studying the Cold Filament 37 profiles from 5 mab to nominally 200 mab were made along the ~200 km-long tow track. This gives an average separation of about 5 km between stations. For comparison each section considered in WK typically had 6–8 stations spaced ~30 km apart.

In the Cold Filament, as pointed out by WK, the bottom layer is the Cold Filament and profiles of potential temperature (θ) made in it have several distinguishable features. The most salient are that the bottom layers in the Cold Filament are anomalously cold[1] ($\theta < 1.82$°C) and are capped with a transition region across which θ changes by several tens of millidegrees Celsius. These features (i.e., relatively cold ($\theta < 1.82$°C) bottom layer and pronounced bottom layer cap ($\Delta\theta > 0.020$ C°) are the criteria used here to identify profiles made in the Cold Filament. Our intent was to make profiles in the lowest 200 m; however, because of time constraints, some profiles were terminated when the bottom layer and its cap were identified.

The first station, 12 (we use the numbering system of the cruise which has a station 31.5, 39a and 39b), was started 0050 GMT 19 June 1981 and the last, 46, ended 1620 GMT 21 June 1981. Thus all 37 stations were made over a 64-hour interval. At each station the deeptow was lowered to 5 mab then raised to nominally 200 mab (or the top of the bottom layer) then lowered to 10 mab to resume the bottom survey. Typically a station took 15–20 minutes to make and variables were sampled every 5 seconds. The up-profiles are primarily considered here since they reached closer to the bottom. The ascent rate (~0.5 m s^{-1}) resulted in a tow-track angle of ~30° to the horizon. This is marginal for lee-effects from the deeptow pressure housing, and some data contamination by the wake of this housing may have occurred. However, as discussed later, the primary differences in up- and down-profiles are consistent with that expected from station-to-station variations and do not appear to be instrumental in origin. We do not think that wake effects for the up-profiles were significant.

Previous CTD studies in the HEBBLE area (e.g., see WK) showed that the CTD conductivity sensor required frequent cleaning to yield stable salinity values. Apparently, without frequent cleaning, sufficient deposition of suspended sediments in the exceptionally turbid bottom layers occurs on the sensor to noticeably affect its characteristics. Because the deeptow CTD was expected to be down continuously for several days with no chance to clean the conductivity sensor, the conductivity data were expected to be inferior to the temperature and pressure data. We do not consider the conductivity data here.

b. Near-bottom currents during the survey

Current meter data from 6 mab during the survey are available at 40°08'N, 62°24'W (WK), about halfway between stations 32 and 37. For the HEBBLE area the current was moderately weak (<5 cm s^{-1}) prior to and during the deeptow survey (Fig. 3). The unfiltered record (not shown) indicates that variability during the survey was predominately due to the semidiurnal, clockwise polarized tide with an amplitude of 5 cm s^{-1}.

c. Temperature data

The potential temperature profiles for each station in Fig. 4 are arranged vertically to show how bottom depth changed along the survey. Generally the depth changes along each leg of the zigzag path are in agreement with the bathymetry of Fig. 2 (this figure is based on data obtained prior to the deeptow-system survey). However, some depth changes are not. For example, station 31, as well as most of the stations at the beginning or end of each long leg, is shallower than one would infer from Fig. 2. As discussed later this is attributed to topographic effects.

As noted in Section 2a, WK inferred that the bounding isotherm for the Cold Filament was θ

[1] That is, they are colder than expected by extrapolation of the vertical temperature gradient of the overlying water. For the lower Scotian Rise this implies the bottom layer temperature $\theta < 1.82$°C.

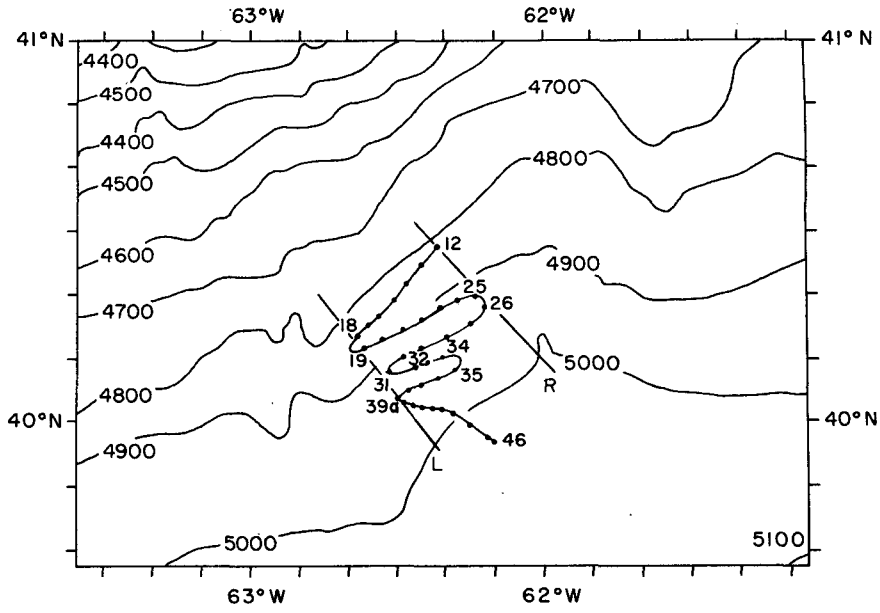

FIG. 2. Topographic map of area based on earlier surveys (courtesy of C. Hollister). Four-digit numbers are isobath depths in meters. Curved, zigzag solid line is deeptow track, and numbered (12–46) dots on it indicate location of profiles shown in Figs. 4 and 8. Straight lines labeled L and R indicate left and right sides of upslope trending channel or thalweg.

= 1.82°C. This isotherm is indicated for the bottom layers in Fig. 5. Bottom layers at stations on the cold side of this isotherm (15–18, 20, 22–29, 31.5–38, 39b–46) have characteristics of the Cold Filament. They are, of course, colder than 1.82°C and have a pronounced cap across which the potential temperature change ($\Delta\theta$) $\geq$ 0.02°C) (Fig. 4). The bottom layers for the remaining stations (i.e., those on the warm side of the 1.82°C isotherm) are not characteristic of the Cold Filament. They are not anomalously cold and their caps are less pronounced ($\Delta\theta$ of the order several 10^{-3} °C) or barely discernible (Table 1 and Fig. 4).

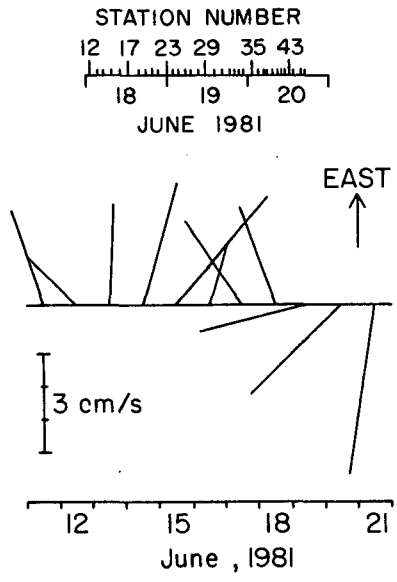

FIG. 3. Stick plot of 24-hour Gaussian filtered current meter record 6 m above the bottom at 40°08'N, 62°24'W prior to 11–17 June and during 18–21 June deeptow survey. Site is about halfway between stations 32 and 37 in Fig. 2.

Figure 5 indicates that a warm (θ > 1.82°C), intrusion extended into the Cold Filament. We do not call it a "meander" because, as pointed out later, it appears to be a consequence of the bottom topography and the moderately weak flow conditions rather than an "instability" in the flow.

Eleven lateral transits across the 1.82°C isotherm in the bottom layer (or equivalently, lateral transits across the Cold Filament) are indicated in Fig. 5. Widths of, and potential temperature contrast across, all 11 transits are listed in Table 2, and an example is shown in Fig. 6. As indicated in Table 2 it is only possible for five of the transits to give an upper bound on the width of the front. For the remaining clearly resolvable fronts, at least half of the temperature variation occurred over a horizontal distance less than 400 m, with this always occurring at the cold side of the front. Thus the upslope edge of the Cold Filament is considerably more front-like than indicated in Fig. 1. If we identify the bounding isotherm of the Cold Filament with 1.81°C rather than 1.82°C, as proposed by WK, the warm intrusion into the Cold Filament would look nearly identical to that seen in Fig. 5, and the width of the front would vary from ~150 m to ~400 m rather than from ~150 m to 4 km (Table 2).

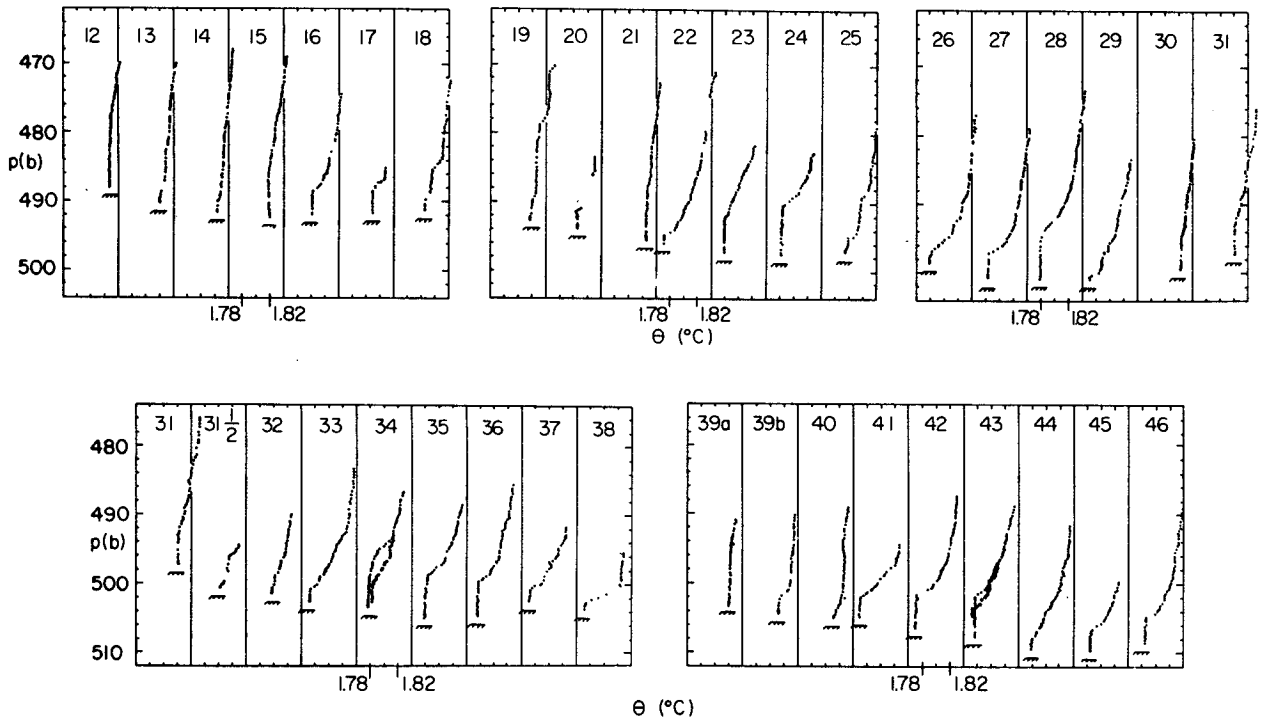

FIG. 4. Potential temperature profiles from the stations indicated in Fig. 2. Double traces for stations 34 and 43 are up-profiles (smaller symbol) and down-profiles (larger symbol).

The Cold Filament bottom-layer thickness decreases as the front is approached (Figs. 4 and 5). This is expected if one identifies the front with the intersection of the Cold Filament cap with the bottom where the Cold Filament disappears by thinning out. This seems reasonable since the temperature contrast across the Cold Filament cap ($\Delta\theta > 0.02$°C, cf. Fig. 4 or WK) is comparable to that across the front (Table 2).

TABLE 1. Listing of bottom-layer potential temperature (θ) and optical transmissivity per meter pathlength of 660 nm light (TRNS) at each station.

	Bottom layer			Bottom layer	
Station	θ (°C)	TRNS (%)	Station	θ (°C)	TRNS (%)
12	1.827	39.4	31	1.821	39.4
13	1.820	39.8	31.5	1.804	38.9
14	1.824	39.4	32	1.798	38.4
15	1.819	39.5	33	1.773	40.4
16	1.801	38.6	34	1.776	39.5
17	1.809	40.0	35	1.779	39.9
18	1.807	37.6	36	1.760	39.2
19	1.818	37.9	37	1.772	40.4
20	1.805	39.7	38	1.771	39.3
21	1.825	39.2	39a	1.821	37.9
22	1.772	39.9	39b	1.812	38.3
23	1.779	38.8	40	1.812	39.3
24	1.781	38.1	41	1.769	39.7
25	1.798	39.2	42	1.771	39.7
26	1.780	39.9	43	1.776	39.6
27	1.784	40.3	44	1.780	39.3
28	1.781	38.2	45	1.784	39.5
29	1.773	40.6	46	1.785	40.0
30	1.823	39.8			

The profile at station 15 (Fig. 4) is unusual in that, in a thermal sense, it is unstably stratified. Of the more than 100 CTD profiles obtained in the HEBBLE area (Weatherly and Kelley, 1981; WK; and Fig. 4), it is the only such bottom layer observed. A stable salinity contrast of about 0.0005‰ uniformly distributed across the this bottom layer, which would not be resolvable with the CTD used, would be sufficient to counter the unstable thermal stratification. However, because of the tight θ–S correlation, even in the bottom layers (WK), we think it unlikely that a counter, restabilizing salinity contrast existed. Using a θ-density relation from data presented in WK (viz. $g\Delta\rho/\rho \approx -0.09\Delta\theta$, where g is gravitational acceleration and ρ is density) to infer a density contrast across this layer, and taking the turbulent diffusivities of heat and momentum both to be $\approx h^2f/(2\pi^2)$ (where h is the layer thickness and f the Coriolis parameter) yields a Rayleigh number $\approx$ 1300. This is somewhat greater than the critical one (1108, Turner, 1973, p. 210) for spontaneous generation of convective motions. This estimate is very uncertain because the effective turbulent diffusivities are difficult to estimate. Finding a supercritical Rayleigh number, however, is consistent with the fact that unstably stratified bottom layers are rarely observed.

The profiles in Fig. 4 were taken as the CTD was

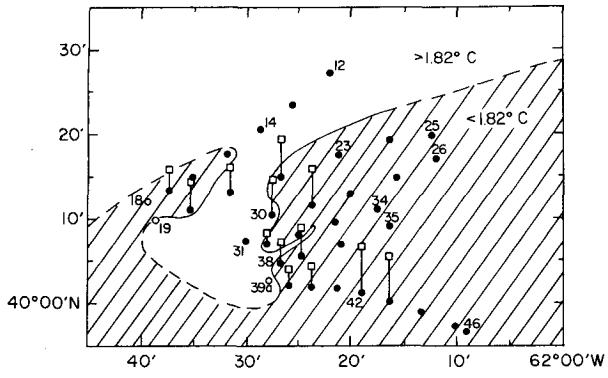

FIG. 5. Plan view of surveyed region showing warm bottom layer intrusion into Cold Filament. Curve is 1.82°C bottom layer isotherm; region where bottom layer temperatures are < 1.82° is shaded. Circles are station locations. The "tethered balloons" above some stations represent the murkier internal layers from group 1 in Table 3. The length of the "tether" is linearly proportional to height above bottom of the internal layer. The "source" bottom layer stations (18, 19, 39a; see text) are indicated by open circles.

raised. Also included in this figure are two down-profiles: for stations 34 and 43. Differences are apparent for the up- and down-profiles at these stations. However, the sense of the change is consistent with what would be expected from the neighboring stations. For example, relative to station 34, the bottom layer at station 33 is thinner and that at station 35 is thicker. Since the up-profile at station 34 was made before the down one, we would expect the former to be thinner than the latter, and it is (Fig. 4). Similarly, one expects and does observe that the up-profile bottom layer thickness is greater than the down-profile bottom layer thickness at station 43 (Fig. 4).

From a temperature section along the total zigzag path with Cold Filament bottom-layer thicknesses superimposed (Fig. 7) one may see several things. One is the previously noted tendency for the Cold Filament bottom-layer thickness to decrease at the edges (i.e., where the 1.82°C isotherm intersects the bottom). Another is that the Cold Filament cap, extending from the top of the bottom layer to approximately the 1.82°C isotherm (Fig. 4), is of comparable thickness to that of the bottom layer (WK previously noted this). Third and most important, there is some correspondence with the location of the Cold Filament Front (the ~1.82°C intersection with the bottom) and local topographic highs. Looking upslope (Fig. 2) one sees that the stations on the left side of the zigzag path (18, 19, 31, 39) and those on the right side (12, 25, 26) are relatively shallow (Fig. 4 or 7). There appears to be a broad channel or thalweg running upslope through the surveyed area. The left and right sides of this thalweg are denoted by lines L and R, and as indicated in Fig. 2, we think the surveyed path crossed the crest of L and reached the left side but not the crest of R. Thus one way of interpreting Fig. 7 is that there was a strong tendency for the Cold Filament to pool within the thalweg.

d. *Transmissometer data*

Profiles of the transmissivity of 660 nm light over a 1-meter path length (TRNS) corresponding to the profiles in Fig. 4 show that, as expected for the moderate currents during the survey, the near-bottom water was moderately turbid (TRNS $\approx$ 40%, Fig. 8). For comparison, clear sea water has TRNS $\approx$ 60%, and during benthic storms in the HEBBLE area (near bottom currents $\geq$ 15 cm s^{-1}, Weatherly and Kelley, 1984), the bottom layers are extremely turbid, TRNS < 20% (e.g., see WK). As noted in WK the bottom-layer thicknesses inferred from the TRNS and θ profiles are in general the same (Figs. 4 and 8). It is above the bottom layer that the profiles sometimes differ markedly in shape.

Often the most turbid water in a particular profile is found not in the bottom layer but in overlying layers (e.g., stations 12–15, Fig. 8). These overlying "murkier" (compared to the local bottom layer) layers are quasi-isothermal (cf. Figs. 4 and 8). Weatherly and Kelly (1982) noted murky (but not murkier than the underlying bottom layer), quasi-isothermal layers above the bottom layer and attributed them to detached bottom layers. They were unable, however, to locate where bottom detachment occurred. For some of the murkier (compared to the local bottom layer) layers, inferences can be made about where they have detached from the bottom. These layers are indicated by brackets for stations 17, 20–22, 25, 27, 29, 31.5, 37, 38, 39b, 40, 42, and 43 in Fig. 8, and their approximated depths, θ and TRNS values given in Table 3.

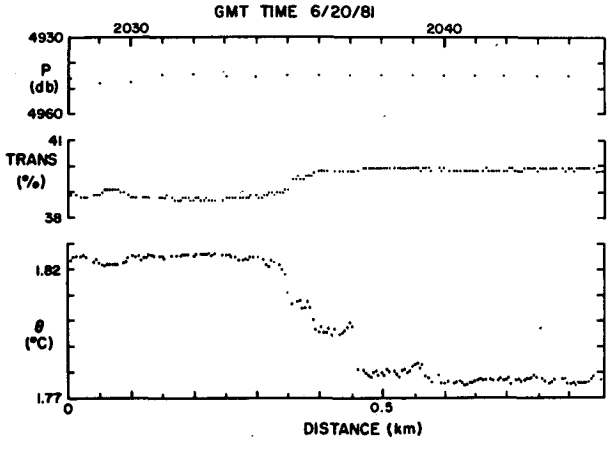

FIG. 6. Pressure (upper panel), optical transmissivity per meter pathlength of 660 nm light (middle panel) and potential temperature records (lower panel) at about 10 m above bottom on deeptow transit from warm (1.82°C) to cold (1.78°C) bottom layer between stations 21 and 22. Pressure record is presented (only every 12th value is plotted) to indicate that changes in transmissivity and temperature are not due to vertical excursion of deeptow.

TABLE 2. Benthic front tabulations.

Benthic front transit	Location between stations	Potential-temperature change (°C)	Horizontal distance between isotherms
1	15 and 16	1.82 to 1.81 1.81 to 1.80	2.3 km 300 m
2	At 19	1.81 to 1.82	<1.2 km†
3	19 and 20	1.82 to 1.81 1.81 to 1.80	3.6 km 150 m
4	20 and 21	1.81 to 1.83	380 m
5	21 and 22	1.82 to 1.78	240 m
6	29 and 30	1.77 to 1.82	370 m
7	31 and 31.5	1.82 to 1.80	<2.4 km††
8	32 and 33	1.80 to 1.81 1.81 to 1.82	<680 m† 110 m
9	32 and 33	1.82 to 1.78	170 m
10	38 and 39a	1.77 to 1.82	<800 m†
11	39a and 40	1.82 to 1.81 1.81 to 1.78	1.4 km <1.0 km*

† Transit occurred as station was made. Horizontal distance traversed while station was made is listed.

†† CTD was towed too high above the bottom to detect transit.

* Transit occurred as station 40 was made. Horizontal distance traversed while station 40 was made is listed.

It is convenient to divide the layers listed in Table 3 into two groups. The smaller, Group 2, consists of stations 25 and 27 which are found near R in Fig. 2 (i.e., on the right side of the thalweg). The other stations, those in Group 1, are closer to L in Fig. 2 (i.e., near the left side of the conjectured thalweg).

The layers in the larger Group 1 in Table 3 all have TRNS = 38.3 ± 0.5%. If these are relic bottom layers, their source bottom layers should have TRNS $\leqslant$ 38.3%. We expect the source bottom layer to be more turbid (i.e., TRNS $\leqslant$ 38.3%) because there is no replacement, once the layer detaches from the bottom, of the suspended sediments which settle out of it. Further, some entrainment of overlying and underlying fluid may occur, and since both are less turbid [the Cold Filament bottom layers are less turbid than the warm intrusion layers (Fig. 8)] this would also tend to reduce the turbidity. Because the density jump capping the Cold Filament bottom layer, which underlies the separated bottom layer, is considerably larger than that capping the warmer source layer, more entrainment of the overlying, warmer fluid rather than the underlying, cooler fluid is expected. Thus, the source bottom layer is expected to be colder and more turbid than the detached layer. Only three stations, 18, 19 and 39a, have bottom layers with TRNS < 38.3% (Table 1). Further, these bottom layers are colder than the detached layers (Tables 1 and 3). These stations are adjacent to the L line in Fig. 2 (i.e., they are near the left rim of the thalweg), as well as being adjacent to the Cold Filament front (Fig. 5). An indicator that the layers in Group 1 have a common source region is that, with one exception, they have approximately the same temperature, 1.828 ± 0.004°C (Table 3). The exception is station 31.5, and its detached layer is the closest to the bottom of all the layers in Group 1 (Table 3 or Fig. 5). Its temperature 1.815°C is intermediate to that of the source stations 18, 19 and 39a and the other layers in Group 2 (Tables 1 and 3). Apparently this detached layer was relatively new and was still in the process of entraining overlying fluid and had not yet reached the ~1.828°C "equilibrium" temperature of the other detached layers in this group. We think entrainment of overlying, clearer water a more likely explanation for the reduced turbidity, compared to the source layer, of the detached layers than sediment settling out of these layers because no clear tendency for decreasing turbidity with increasing distance from the source region is apparent in Table 3.

The detached layers of Group 2 are more turbid (TRNS = 37.4%) and cooler (θ = 1.820 ± .004°C) than those in Group 1 (Table 3). They are also more turbid than any of the bottom layers in the surveyed region (Table 1), and hence their source region is probably outside the surveyed region. There is some suggestion in the data that a second source region may exist to the northeast of stations 25 and 27 (i.e., near the line R in Fig. 2 or the right side of the conjectured thalweg). The 1.82°C isotherm in Fig. 7 is seen to dip towards the bottom as the bottom-layer source region for the Group 1 detached layers, stations

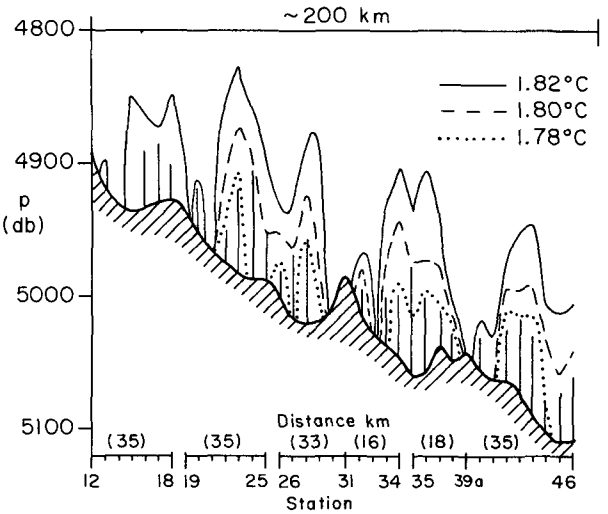

FIG. 7. Potential temperature transect along the zigzag deeptow path. The stations are indicated as uniformly spaced. Thickness of Cold Filament bottom layers indicated by vertical lines.

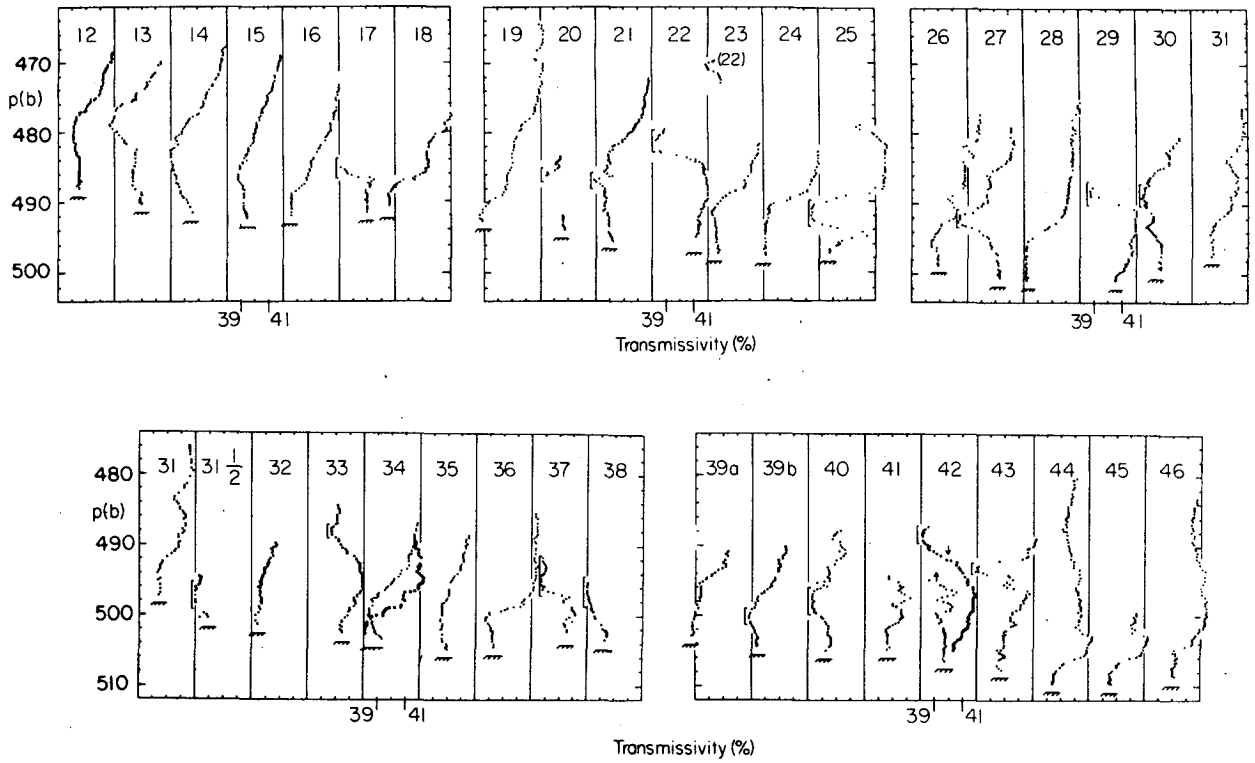

FIG. 8. Profiles of optical transmissivity per unit path length of 660 nm light at the stations in Fig. 2. Up-profiles (smaller symbol) and down-profiles (larger symbol) are shown at stations 34 and 42. Vertical lines along selected parts of the profiles at stations 17, 20–22, 25, 26, 27, 29, 31.5, 33, 37, 39b, 40, 42, 43 are the Group 1 layers of Table 3.

18, 19 and 39a, is approached. Similarly, as stations 25 and 27 are approached the 1.82°C isotherm begins to dip towards the bottom.

TABLE 3. Approximate midpoint potential temperature (θ), optical transmissivity per meter pathlength of 660-nm light (TRNS) and depth of murkier (than local bottom layer) detached bottom layers indicated by bracketed vertical line in Fig. 9.

		Detached bottom layer approximate midpoint		
Station	Group	θ (°C)	TRNS (%)	Depth (db)
17	1	1.828	38.0	4850
20	1	1.828	38.4	4860
21	1	1.830	37.8	4878
22	1	1.828	38.2	4820
25	2	1.816	37.4	4915
27	2	1.824	37.4	4920
29	1	1.829	38.8	4885
30	1	1.832	38.5	4890
31.5	1	1.815	38.0	4975
37	1	1.825	38.8	4940
38	1	1.828	38.0	4960
39b	1	1.828	37.8	5000
40	1	1.827	38.3	4980
42	1	1.829	38.1	4890
43	1	1.831	38.0	4935

3. Regional survey of the cold filament

Hydrographic sections made in the western portion of the North American Basin are now examined to see where a Cold Filament-like feature is seen in the North American Basin. As noted earlier, WK found something like the Cold Filament in historical sections from 50 to 72°W (Fig. 9, dashed sections), essentially along the northern rim of the North American Basin. The present survey examines hydrographic transects along 15 sections (Fig. 9, solid sections) not considered by WK; seven are equatorward and one is eastward of those examined by WK.

More sections exist than are examined here. However, those excluded from discussion were judged unsuitable for detecting the Cold Filament which is only about 60-m thick (or about 150 m if its cap is included), 100 km wide and found at the base of the rise. For example, seven of the sections are from Gulf Stream '60 (Table 4). Those Gulf Stream '60 sections not presented had an insufficient number of near-bottom samples at the base of the rise to detect the presence of the Cold Filament.

Most of the sections are of *in situ* temperature. Partly because of this, and partly because of the contouring intervals, it is not apparent if all these sections reveal a Cold Filament-like feature. Thus we decided to estimate θ sections from the *in situ* tem-

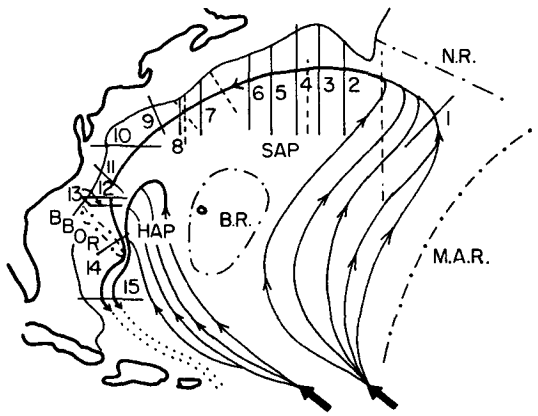

FIG. 9. Sketch of North American Basin showing locations of sections, (numbered solid lines) listed in Table 4. Dashed sections were considered in WK. The Mid-Atlantic Ridge (MAR), Newfoundland Ridge (NR), Bermuda Ridge (BR) and Blake-Bahama Outer Ridge (BBOR) are indicated by dot-dashed lines. HAP and SAP represent Hatteras Abyssal Plain and Sohm Abyssal Plain, respectively. See text for discussion of arrowed and dotted lines.

perature sections. For the cases when pressure was not listed in the original station data, CTD station 22 in WK was used to establish a depth–pressure relationship for computing θ. The resulting θ-sections (Fig. 10, Sections 2–13, 15) all show a Cold Filament-like feature approximately where anticipated and of expected dimensions. Two, Sections 2 and 9, have two "pools." Weatherly and Kelly (1982) noted a similar occurrence on one of their sections and thought it might be due to a meander in the Cold Filament or to it pinching off with a new one following. The results of the previous section suggest it could also be due to a cast being made into a warm intrusion.

Sections, 1 and 14a, are presented in the references (Table 4) as potential temperature sections. Since both clearly indicate something like the Cold Filament with expected dimensions and location, we do not reproduce them in Fig. 10. The latter transect is unlike all the other sections in that on the seaward side of the Cold Filament-like "pool" the isotherms do not intersect the bottom. We attribute this to a confluence with the Cold Filament of a cyclonic abyssal flow pattern on the Hatteras Abyssal Plain; such a confluence is proposed later to account for the Cold Filament's lower temperature south of about 36°N.

The θ-transects along section 14 shown by Mills and Rhines (1979) do not reveal the Cold Filament. However, the contouring in their figures is sufficiently coarse to mask it. We noticed that with some of the sections in WK the Cold Filament would not appear when contoured with a comparable resolution. We

TABLE 4. References for numbered sections shown in Fig. 10. Depth and temperature of Cold Filament-like feature seen in references (Sections 1 and 14) or in Figs. 11 and 12 are listed.

Section	Cold filament depth (m)	Cold filament θ (°C)	Reference	Location
1	4800	<1.8	Section 7 of Worthington (1976)	~46°W
2	5000 5300	1.75 1.75	Fuglister (1963)	52°30'W
3	5000	1.78	Fuglister (1963)	54°30'W
4	4900	1.80	Fuglister (1963)	56°30'W
5	5100	1.76	Fuglister (1963)	58°30'W
6	4400	1.81	Fuglister (1963)	60°30'W
7	4800	1.81	Fuglister (1963)	64°30'W
8	4700	1.80	Fuglister (1963)	66°30'W
9	4700 5100	1.83 1.79	Worthington and Wright (1970)	Off Cape Cod
10	4600	1.83	Fuglister (1960)	36°N
11	5000	1.75	Richardson (1977) Fig. 2	Off Cape Hatteras
12	4900	1.75	Swallow and Worthington (1961)	33°N
13	5000	1.75	Swallow and Worthington (1961)	Off Cape Romain
14a	5200	1.68	Amos *et al.* (1971)	30.5°N
b	5150	1.70	Mills and Rhines (1979) Oceanus 31 data	30°N
c	5200	1.68		31°N
15	5500	1.60	Fuglister (1960)	24°N

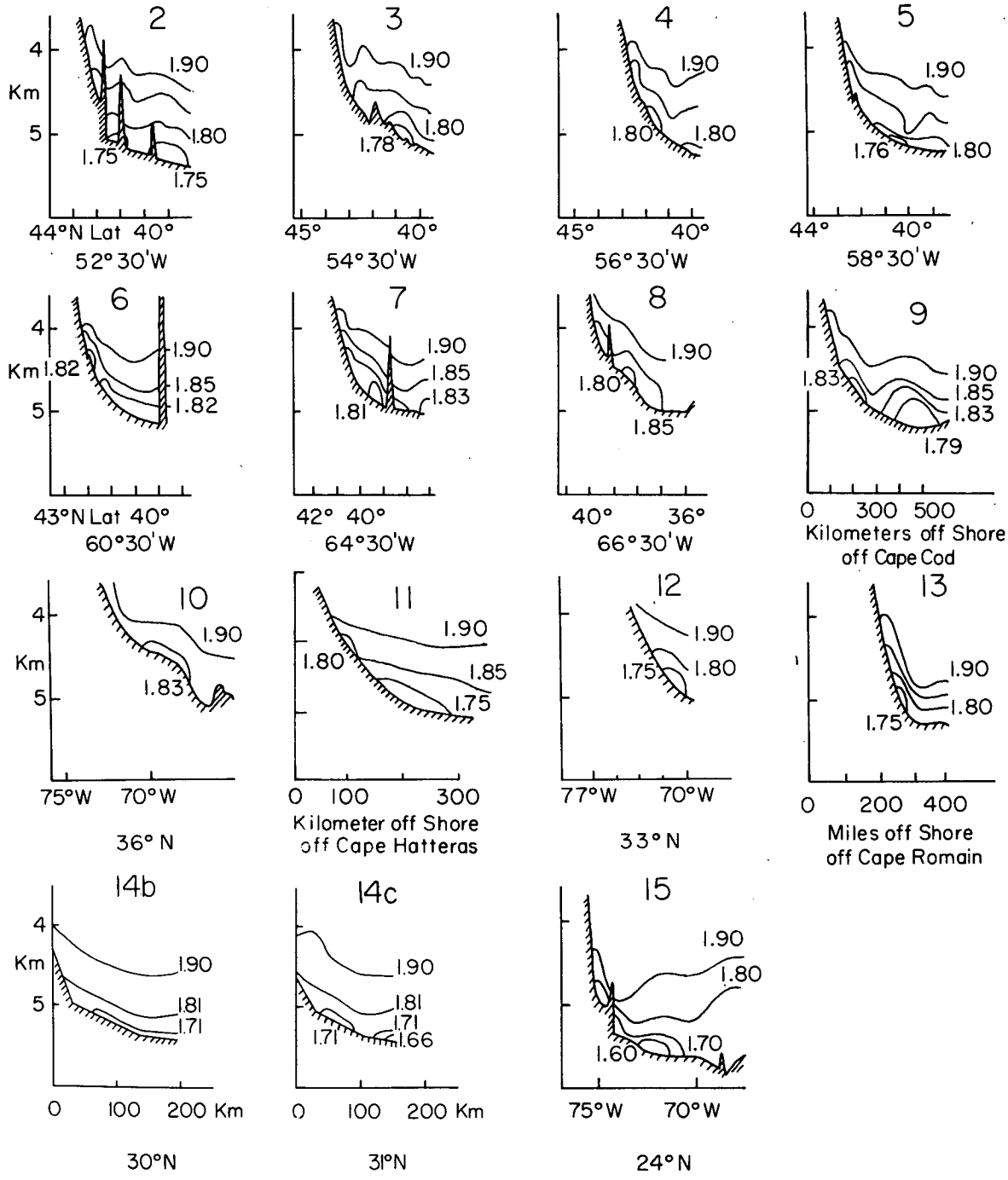

FIG. 10. Inferred near-bottom potential temperature transects for indicated sections in Table 4, 2–13, 15, and re-done θ-sections from data presented by Mills and Rhines (1979), Sections 14b, c.

thus replotted these transects with finer resolution from listings of the original data. One of the sections, that made from the R.V. *Atlantis II* Cruise 100, is not shown because no data within 100 m of the bottom were taken in the region of interest (the Cold Filament is about 100 m thick). Section 14b (Fig. 10), like Section 14a, does not have the isotherms intersecting the bottom on the seaward side. As for Section 14a, we attribute this to confluence with a cyclonic flow pattern on the Hatteras Abyssal Plain. While no "pool" is indicated, vertical θ-profiles (not reproduced here) show that, as expected, the bottom layers are "too cold" (see footnote 1) where we identify the Cold Filament in this transect (Table 4).

Section 14c (Fig. 10) clearly shows a Cold Filament-like feature; θ-profiles for this transect (not shown here) also show the bottom layers in it to be "too cold."

From the sections listed in Table 4, the Cold Filament appears to warm as it flows along the northern rim of the North American Basin (Fig. 11). If real, the warming could be due to lateral mixing with warmer water, or entrainment of warmer overlying water. We think the latter is less likely since, as pointed out by WK, the large Richardson number of the Cold Filament cap should greatly inhibit vertical mixing. However, as noted later, this heating trend may not be real.

A pronounced cooling trend occurs south of 36°N along the western rim of the basin (Table 4 and Fig. 11). We suspect it to be real and due to confluence with colder, θ = 1.60°C, water flowing equatorward on the western margin of the Hatteras Abyssal Plain. Amos *et al.* (1971) and Tucholke *et al.* (1973) inferred a near-bottom cyclonic flow of water of about this temperature around the Hatteras Abyssal Plain.

4. Summary and conclusions

a. Local survey

CTD and optical transmissivity data obtained in a detailed bottom survey (Shor and Lonsdale, 1981) have permitted a more detailed examination of the upslope half of the Cold Filament than previously available (WK). To incorporate a Cold Filament investigation as part of the bottom survey, vertical profiles were made about every 5–6 km along the ~200 km-long survey path (Fig. 2) from ~5 mab to ~200 mab, and in some cases only to the top of the bottom layer. These data indicate that the Cold Filament was there (Fig. 5). This, together with the results of the regional survey (Section 3), reinforce WK's conclusion that the Cold Filament is a permanent feature found at the base of the rise along major portions of the western rim of the North American Basin.

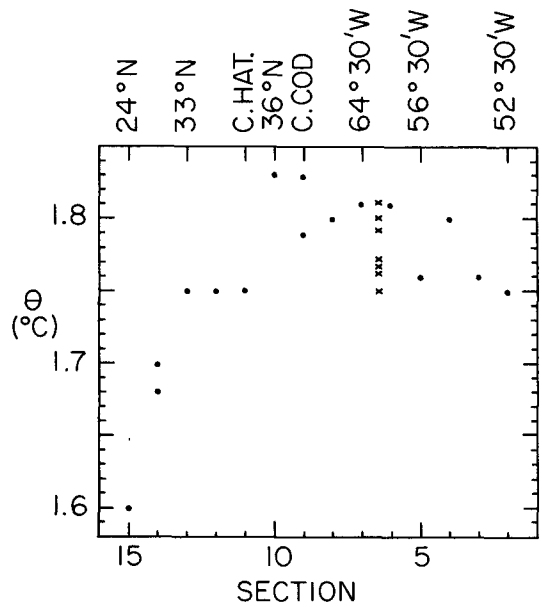

FIG. 11. Cold Filament temperature as a function of section number. Dots are from sources listed in Table 4; crosses are values from WK.

Lateral transits across the Cold Filament's upslope edge show it to be considerably sharper than indicated in WK (Fig. 1). This benthic front (if we identify the bounding isotherm for the Cold Filament as 1.81°C rather than the 1.82°C used by WK) has a width ranging from 150 m to about 400 m where the temperature changes by ~10 to 40°mC (Table 2). [Using 1.82°C as a bounding isotherm gives a width ranging from 150 m to about 4 km with a temperature contrast ranging from ~20 to ~50°mC (Table 2).] What distinguishes this benthic front from others, either comparably strong ones (Armi and D'Asaro, 1980; McCave *et al.*, 1982) or weaker ones (Thorpe, 1983), is that it is a permanent abyssal feature.

During the moderately weak flow conditions during the survey (Fig. 3), the upslope portion of the Cold Filament apparently pooled or settled into a broad (35 km wide), shallow (~30 m relief) channel or thalweg which trended up-downslope. If this indeed was the case, we would expect the buoyancy term in the bottom boundary-layer momentum equations (cf. Bird *et al.*, 1982) to be of the same order as the frictional term, or their ratio $(\alpha g \Delta\rho/\rho)(u_*^2/h)$ = O(1). Here, α is the slope of the thalweg's sides, g gravity, $\Delta\rho/\rho$ the density contrast across the Cold Filament bottom layer cap, u_* the friction velocity and h is the Cold Filament bottom-boundary-layer thickness. With $\Delta\rho/\rho = 4 \times 10^{-6}$ and h = 60 m (WK), u_* = 0.04 × (the free-stream velocity) (Weatherly, 1984), and the free-stream velocity ~0.04 m s^{-1} (Fig. 3), this ratio = 1.8 = O(1), for α = 30 m/(35/2 km). That the Cold Filament bottom-layer thickness tended to be thinner near the edges of the thalweg (lines L and R in Fig. 5) and thicker in between (Fig. 7) is also consistent with the proposed pooling.

A bottom-layer source region for some of the observed detached, relic bottom layers was identified (Table 3, Group 1). This source region is about the left side of the thalweg (line L in Fig. 2) near stations 18, 19 and 39a. Some entrainment primarily of overlying fluid was proposed to account for these detached layers being somewhat warmer and less turbid than the source layers. The large density jump separating the detaching layer from the underlying Cold Filament bottom layer should inhibit entrainment at the lower boundary of the detaching layer. An example of a separating bottom layer can be seen in the last panel of Fig. 8. The source bottom layer

is at station 39a, and the relatively turbid (compared to the local bottom layer) detached layer (indicated by a bracket) is seen to tend to drift farther from the bottom as the distance from the source increases (stations 39b, 40, 42 and 43). The horizontal extent of the detached layer is limited since it is not seen at stations 44 and 46.

The results of the small-scale survey of the Cold Filament bear upon the High Energy Benthic Boundary Layer Experiments (HEBBLE) (e.g., Shor and Lonsdale, 1981) because the HEBBLE site (40°26'N, 62°21'W) is approximately station 12 (Fig. 2). Our study reveals that since this site is close to the upslope edge of the Cold Filament, it is also close to a permanent benthic front. We have seen in this study that bottom layer detachment is favored at this front. This front must wander back and forth over the site since we have seen that its location is determined, at least during moderately weak flow conditions, by the strength of the current and the slope of the thalweg's side. When the front is directly over the HEBBLE site we would expect the bottom layer to be very stably stratified. Thus the HEBBLE site is an unusual one since detaching bottom layers and stably stratified bottom layers are not uncommon there because of the proximity to the front.

b. Regional survey

The historical hydrographic transects examined here (Table 4), together with those examined in WK, indicate that the Cold Filament extends along the northern and western edges of the North American Basin from 46°W (south of the Newfoundland Ridge) to at least 24°N, and perhaps to 20°N, along the continental rise (Fig. 9).

The data in Table 4 indicate that along the northern rim, between ~52 and ~70°W its temperature increases (Fig. 11). However, whether this heating trend is real, or due to limited sampling (only one transect per section) is unclear. WK noted that at ~62°W the Cold Filament temperature ranged from 1.75°C to 1.81°C in the eight sections they made. This practically encompasses the temperature range seen in Table 4 between the Newfoundland Rise and about 36°N.

The region along the northern rim is also one of large abyssal eddy kinetic energy (e.g., Weatherly, 1984), and how the Cold Filament can maintain its identity there is unclear. Kelley (1984) noted, however, that rather than being disrupted or disorganized by overhead passage of Gulf Stream meanders and rings it appears to be displaced up- and downslope. We note that other narrow, thin features such as "meddies" (e.g., McDowell and Rossby, 1978) maintain their identities over long distances.

South of ~36°N a cooling trend is indicated (Fig. 11). We think, assuming the Cold Filament still flows equatorward in this region, that this is real and due to the confluence of colder ($\theta \approx 1.60$°C) Antarctic Bottom Water (AABW) which Amos *et al.* (1971) and Tucholke *et al.* (1973) have suggested flows cyclonically about the Hatteral Abyssal Plain. Two of the three Cold Filament-like "pools" along section 14 suggest that such a confluence may occur; the isotherms do not intersect the bottom on its seaward side on these two transects. The examined transects (Table 4) do not have adequate horizontal resolution to conclude whether the width and/or thickness of the Cold Filament increases south of ~36°N, consistent with the suggested confluence.

What happens to the Cold Filament south of 24°N is unclear. One potential temperature section by Tucholke *et al.* (1973) (their section 2) together with one of their current meter records (the six-month record from their mooring E) indicate cold ($\theta \approx 1.55$–1.60°C) bottom water flowing equatorward through the Vema Gap. Farther to the south Tucholke and Eittreim (1974) observed a relatively turbid layer, with $\theta \approx 1.6$°C, crossing the Puerto Rico Trench and then extending easterly and southeasterly at about 5000 m depth along the south flank of this trench. This layer became less turbid progressing from west to east and at about 19°N, 62°W it was barely discernable. The Cold Filament is a relatively turbid layer on the Scotian Rise (e.g., see WK) but whether it remains so for the sections equatorward of Section 8 in Fig. 9 is unknown. Biscaye and Eittreim (1977) show relatively turbid bottom layers all along the western side of the North American Basin. We suspect that Tucholke and Eittreim (1974) may have observed a continuation of the Cold Filament.

Based on data discussed here and in WK, we have sketched, in Fig. 9, a tentative flow pattern of near-bottom AABW[2] in the North American Basin. We stress that it is a tentative sketch and note that any resemblance to the southern-source flow pattern of Stommel *et al.* (1958) is not coincidental. Current meter data from the Ceara and Demerara Abyssal Plains reported by Whitehead and Worthington (1982) indicate about 1×10^6 m^3 s^{-1} (1 Sv) of AABW enters the North American Basin from the south. This is indicated by the two thicker, northwestward pointing arrows in the lower right corner of Fig. 9. Part of this northward flow proceeds west of the Bermuda Rise, then flows cyclonically about the Hatteral Abyssal Plain, and by the time it is adjacent to the Blake–Bahama Outer Ridge it is flowing southward. As it flows northward we suspect it is a broad, slow flow, and when it flows southward we suspect it is more

[2] Whitehead and Worthington (1982) call all water with $\theta < 1.9$°C in the western North Atlantic, AABW. Here bottom flow of AABW in the North American Basin is taken to be bottom layers with $\theta < 1.82$°C.

organized and stronger, i.e., a deep western-boundary current. This is essentially the deep flow pattern for the Hatteras Abyssal Plain proposed by Amos *et al.* (1971) and Tucholke *et al.* (1973). As indicated in the former reference (their Fig. 12) we suspect the organized, equatorward flowing portion of this flow is just seaward of the 5000 m isobath. Part of the northward flowing AABW entering the North American Basin flows northward between the Bermuda Rise and the Mid-Atlantic Ridge.[3] As it moves northward we expect it to be a very broad slow flow. However, we expect it to organize into the Cold Filament somewhere south of the Newfoundland Ridge and to begin flowing equatorward along the continental rise at or somewhat seaward of the 4900 m isobath. Thus we suspect the Cold Filament is a deep western boundary current associated with a southern source of AABW. In the vicinity of the Blake–Bahama Outer Ridge we think it merges with the equatorward flow on the western edge of the Hatteras Abyssal Plain. Weatherly and Kelly (1982) estimated a Cold Filament volume transport of about 0.5×10^6 m^3 s^{-1} south of Nova Scotia. To match the previously noted 1 Sv flow of AABW entering the North American Basin from the south, about 0.5 Sv should enter the Hatteras Abyssal Plain form the south so that the combined equatorward flow at about 24°N should be about 1 Sv. How far south of 24°N it extends is unclear as indicated by the dotted portion south of 24°N in Fig. 9.

The deep western boundary current in the North American Basin associated with Norwegian Sea Overflow Water flows along the continental slope at or above the 4000 m isobath (Hogg, 1983). This warmer ($\theta > 1.9$°C) flow continues equatorward into the Guiana Basin and crosses the equator into the South Atlantic (Warren, 1981). We do not expect the same to occur for the Cold Filament. We think it is a source–sink flow limited to the North American Basin and perhaps the northern portion of the Guiana Basin. We do not expect it to continue to the vicinity of its source, i.e., where AABW enters the western North Atlantic. We suspect that, consistent with ideas of deep western boundary currents (e.g., Warren, 1981), it tends to dissipate (i.e., to be "leaky" to the ocean interior) all along its path. Results presented by Tucholke and Eittreim (1974) suggest that its vestiges are seen south of about 20°N along the western and southern portions of the North American Basin.

If there is a broad poleward slow flow of AABW in bottom layers on the Hatteras and Sohm Abyssal Plains (Fig. 9), the observations of Armi and D'Asaro (1980) of benthic fronts in bottom layers and of Ebbesmeyer *et al.* (1983) of a 200 km-wide cold ($\theta = 1.6$°C) bottom "parcel" indicate that the flow may occur in isolated "blobs" rather than spread uniformly over the abyssal plains. This may be the reason why, as pointed out in WK, not all observed bottom layers on abyssal plains in the western North Atlantic are anomalously cold (i.e., colder than expected by extrapolation from overlying water). Profiles made into an AABW parcel would reveal an anomalously cold bottom layer, those made outside would not.

While it may be long (perhaps as long as 5000 km), moderately broad (about 100 km wide) and transporting on the order of 1 Sv, the Cold Filament's thinness (about 100 m thick) and remoteness (at about 5000 m depth on the continental rise) give it the semblance of a curiosity. While it may be of doubtful significance, its dynamic signature extends at times from the bottom to about 2000 m depth (Fig. 12). It is interesting that Ebbesmeyer *et al.* (1983) also found isopycnal doming, in their case above a bottom parcel on the Hatteras Abyssal Plain, up to 2000 m depth.

We again stress that the bottom layer circulation pattern in Fig. 9 is speculative. This is in part a reflection of a lack of consensus, due to limited data, concerning some basic aspects of the abyssal circulation in the western North Atlantic. For example, whether the abyssal circulation about the Hatteras and Sohm Abyssal Plains is cyclonic or anticyclonic is unclear. For the latter, Amos *et al.* (1971), Tucholke *et al.* (1973) and McWilliams (1983) have suggested

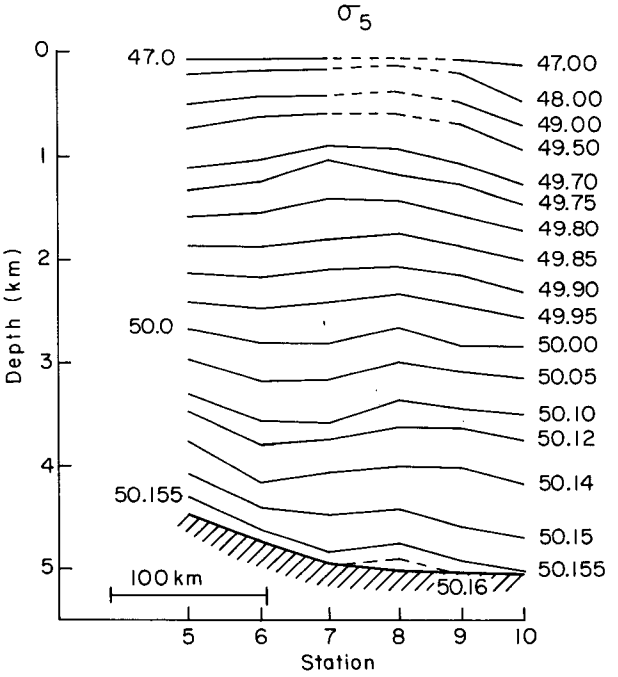

FIG. 12. Full water column density (σ_5) section for the transect shown in Fig. 1.

[3] That AABW flows northward both west and east of the Bermuda Rise is seen clearly in Plate 19 of Worthington and Wright (1970).

a cyclonic pattern, while Hogg (1983) indicates an anticyclonic pattern. For the Sohm Abyssal Plain Hogg (1983) infers a cyclonic flow while McWilliams (1983) an anticyclonic one.

For the Hatteras Abyssal Plain we favor a cyclonic pattern for abyssal flows on the lower continental margin. However, we are unaware of any long-term current meter records to substantiate this. Thus it is certainly possible, as suggested by a reviewer, that in this region the cold filament feature may be flowing poleward. If this is indeed the case then this implies three things: 1) that the southward flowing Cold Filament in the Sohm basin does not continue into the Hatteras basin as shown in Fig. 9, 2) that the previously noted cooling trend in the Hatteras basin (Table 4 and Fig. 11) is actually a heating trend due probably to lateral mixing, and 3) that the heating trend indicated for the Sohm basin in Table 4 is real and not an artifact of aliased sampling.

For the Sohm basin we and Hogg (1983) both suggest a westward abyssal flow on the lower continental rise. There are ample long-term current observations to substantiate this (e.g., Hogg, 1983). We imply here that the portion of this flow upslope of about the 4900 m isobath (the Cold Filament is centered about this isobath) continues into the Hatteras basin. Hogg (1983) indicates all this flow is recirculating back onto the Sohm Abyssal Plain. Hogg's flow scheme is driven by fluctuations in the upper ocean similar to that predicted in numerical models (e.g., Holland, 1978) while ours is postulated as a source–sink flow. We do not imply that Hogg's or our flow schemes are mutually exclusive; either or both may be occurring. We think the Cold Filament extends along the northwestern edge of the Sohm Abyssal Plain onto the western edge of the Hatteras Abyssal Plain, rather than recirculates back onto the Sohm Abyssal Plain and that there are thus two distinct Cold Filament-like features in each basin. This is because in the Sohm basin the Cold Filament is centered about the 4900 m isobath, which is the deepest isobath connecting the basins along the continental rise. We think it reasonable that there is recirculation of abyssal flows seaward of the 4900-m isobath in the Sohm basin.

Long-term current meter observations at a depth of about 4900 m on the western sill between the Sohm and Hatteras Abyssal Plains, as well as on the lower continental rise in the Hatteras basin are needed to determine whether the Cold Filament does extend equatorward in a continuous manner south of ~36°N to join up with a similar, but slightly deeper and colder, equatorward flow as sketched in Fig. 9.

Acknowledgments. We thank P. Lonsdale for agreeing to make the vertical profiles during the deeptow survey and R. Flood for providing listings of the deeptow data. T. Joyce, P. Rhines and R. Millard Jr. were very helpful in providing some of the historical hydrographic data. We profited from comments by D. Nof, W. Sturges III and B. Warren during the research and from C. Hollister, I. McCave, R. Romea, and the reviewers to the manuscript. This work was done as part of the High Energy Benthic Boundary Layer Experiments (HEBBLE) Program under Contract N00014-82-0404 with the Office of Naval Research.

REFERENCES

Amos, A. F., A. L. Gordon and E. D. Scheider, 1971: Water masses and circulation patterns in the region of the Blake–Bahama Outer Ridge. *Deep-Sea Res.*, **18,** 145–166.

Armi, L., and E. D'Asaro, 1980: Flow structures of the benthic ocean. *J. Geophys. Res.*, **85,** 469–484.

Bird, A. A., G. L. Weatherly and M. Wimbush, 1982: A study of the bottom boundary layer over the Eastward Scarp of the Bermuda Rise. *J. Geophys. Res.*, **87,** 7944–7954.

Biscaye, P. E., and S. L. Eittreim, 1977: Suspended particulate loads and transports in the nepheloid layer of the abyssal Atlantic Ocean. *Mar. Geol.*, **23,** 155–172.

Ebbesmeyer, C. C., B. A. Taft, J. C. McWilliams, C. Shen, S. C. Riser, H. T. Rossby, P. E. Biscaye and H. G. Ostlund, 1985: Variability of physical and chemical properties along a northwestern Atlantic oceanographic section (23°–33°N, 70°W) during April 1977. Submitted to *J. Phys. Oceanogr.*

Fuglister, F. C., 1960: Atlantic Ocean atlas of temperature and salinity profiles and data from the International Geophysical Year of 1957–1958. *Woods Hole Oceanographic Institution Atlas Series,* Vol. 1, 209 pp.

——, 1963: Gulf Stream '60. *Progress in Oceanography,* Vol. 1, Pergamon, 265–373.

Hogg, N. G., 1983: A note on the deep circulation of the western North Atlantic: Its nature and causes. *Deep-Sea Res.*, **30,** 945–962.

Holland, W. R., 1978: The role of mesoscale eddies in the general circulation of the ocean—Numerical experiments using a wind-driven quasi-geostrophic model. *J. Phys. Oceanogr.*, **8,** 363–392.

Kelley, E. A., Jr., 1984: A study of highly energetic near-bottom flow at the base of the Scotian Rise. Ph.D. dissertation, Dept. of Oceanogr., Florida State University, 108 pp.

McCave, I. N., C. D. Hollister, E. P. Laine, P. F. Lonsdale and M. J. Richardson, 1982: Erosion and deposition on the eastern margin of the Bermuda Rise in the late Quaternary. *Deep-Sea Res.*, **29,** 535–561.

McDowell, S. E., and H. T. Rossby, 1978: Mediterranean water: An intense mesoscale eddy off the Bahamas. *Science,* **202,** 1085–1087.

McWilliams, J. C., 1983: On the mean dynamical balances of the Gulf Stream Recirculation Zone. *J. Mar. Res.*, **41,** 427–460.

Mills, C. A., and P. Rhines, 1979: The deep western boundary current at the Blake–Bahama Outer Ridge: Current meter and temperature observations. Tech. Rep. WHOI-79-85, Woods Hole Oceanographic Institution, 77 pp.

Richardson, P. L., 1977: On the crossover between the Gulf Stream and Western Boundary Undercurrent. *Deep-Sea Res.*, **24,** 139–159.

Shor, A., and P. Lonsdale, 1981: HEBBLE Site characteristics: Downslope processes on the Nova Scotia Lower Continental Rise, *Trans. Am. Geophys. Union,* **62,** 892.

Spiess, F. N., and J. D. Mudie, 1970: Small-scale topographic and magnetic features. *The Sea,* Vol. 4, A. E. Maxwell, Ed., Wiley and Sons, 205–250.

Stommel, H., A. Arons and A. Faller, 1958: Some examples of stationary planetary flow patterns in bounded basins. *Tellus,* **10,** 179–187.

Swallow, J. C., and L. V. Worthington, 1961: An observation of a deep counter-current in the western North Atlantic. *Deep-Sea Res.*, **8**, 1–19.

Thorpe, S. A., 1983: Benthic observations on the Madeira Abyssal Plain: Fronts. *J. Phys. Oceanogr.*, **8**, 1430–1440.

Tucholke, B. E., and S. Eittreim, 1974: The Western Boundary Undercurrent as a turbidity maximum over the Puerto Rico Trench. *J. Geophys. Res.*, **27**, 4115–4118.

——, W. R. Wright and C. D. Hollister, 1973: Abyssal circulation over the Greater Antilles Outer Ridge. *Deep-Sea Res.*, **20**, 973–995.

Turner, J. S., 1973: *Buoyancy Effects in Fluids.* Cambridge University Press, 367 pp.

Warren, B. A., 1981: Deep circulation of the world ocean. *Evolution of Physical Oceanography,* B. A. Warren and C. Wunsch, Eds., The MIT Press, 6–41.

Weatherly, G. L., 1984: An estimate of bottom friction dissipation by Gulf Stream fluctuations. *J. Mar. Res.*, **42**, 289–301.

——, and E. A. Kelley, Jr., 1981: An analysis of hydrographic data from *Knorr* Cruise 74 in the HEBBLE area September–October, 1979. Dept. of Oceanogr. Tech. Rep., Florida State University, 38 pp.

—— and ——, 1982: "Too cold" bottom layers at the base of the Scotian Rise. *J. Mar. Res.*, **40**, 985–1012.

——, and ——, Jr., 1984: Storms and flow reversals at the HEBBLE Site. *Mar. Geol.*, (in press).

Whitehead, J. A., and L. V. Worthington, 1982: The flux and mixing rates of Antarctic Bottom Water within the North Atlantic. *J. Geophys., Res.*, **87**, 7903–7924.

Worthington, L. V., 1976: *On the North-Atlantic Circulation.* The Johns Hopkins Press, 110 pp.

——, and W. R. Wright, 1970: North Atlantic Ocean atlas of potential temperature and salinity in the deep water, including temperature, salinity and oxygen profiles from the *Erika Dan* cruise of 1962. *Woods Hole Oceanographic Institution Atlas Series,* Vol. 2, 58 plates.